Thermodynamics of flip-flop and desorption for a systematic series of phosphatidylcholine lipids†

Nicolas Sapay,‡ W. F. Drew Bennett‡ and D. Peter Tieleman*

Received 4th February 2009, Accepted 6th April 2009
First published as an Advance Article on the web 21st May 2009
DOI: 10.1039/b902376c

We have investigated the thermodynamics of phospholipid flip-flop and desorption. Using a series of PC (phosphatidylcholine) lipids with different lengths of acyl tails, and number of unsaturated tails, we calculated potentials of mean force (PMFs) in atomistic molecular dynamics simulations. The PMFs describe the free energy for moving a single lipid molecule from water to the center of the respective lipid bilayer. The free energy to move the lipid from equilibrium to the bilayer center is assumed to be the free energy barrier for lipid flip-flop. We find that the free energy barrier for flip-flop is strongly dependent on the structure of the bilayer; ranging from 16 kJ mol^{-1} in the thin DLPC bilayer, to 90 kJ mol^{-1} in the DOPC bilayer. There are large deformations in the bilayers' structure, to accommodate the charged PC head group in the bilayer interior. We observe pore formation in all the bilayers, except for POPC and DOPC. The free energy for desorption is equal to the excess chemical potential of the lipid in the bilayer compared to bulk water. The increased chemical potential for PC lipids with longer acyl tails is in qualitative agreement with the critical micelle concentrations. We also determined PMFs for transferring water into the center of the series of lipid bilayers. Water has the same free energy of transfer to the center of all the bilayers, indicating the lipid PMFs differ due to bilayer deformations. Lipid bilayers are soft and deformable, allowing large structural changes, which are dependent on the composition of the bilayer. Our results show that similar PC lipids with only slightly different acyl tails, can have dramatically different thermodynamic behavior.

Introduction

Cellular membranes are heterogeneous in composition and structure. For example, endoplasmic reticulum (ER) membranes have a symmetric distribution of lipids between the two leaflets of the bilayer, while eukaryotic plasma membranes have an asymmetric distribution of lipids, with phosphatidylserine (PS) and phosphatidylethanolamine (PE) enriched on the intracellular leaflet, and phosphatidylcholine (PC) and sphingomyelin (SM) enriched on the extracellular leaflet.[1] Most phospholipids are synthesized on the cytoplasmic leaflet of the ER,[1] so flip-flop is required to allow uniform growth of the membrane and for lipids destined for the extracellular leaflet of the plasma membrane.

Due to the slow rate of passive flip-flop for PC lipids across model bilayer systems,[2–4] it is generally accepted that the process is protein mediated. For a review of current lipid translocators see ref. 5. Exposure of PS to the outside of the cell has been implicated in blood coagulation and apoptosis.[5] Specific aminophospholipid flippases have been identified as P4-ATPases[5] for the eukaryotic plasma membrane, suggesting passive flip-flop is a natural process cells must fight against to maintain asymmetric lipid distributions. No dedicated ER lipid translocator has been clearly identified in spite of several attempts.[6] It has been shown that the rate of phospholipid flip-flop can be enhanced by the presence of model peptides[7] and α-helical integral membrane proteins,[8] in an energy independent fashion. It has been postulated that the ER membrane has the intrinsic ability to equilibrate lipids between leaflets due to the presence of non-specific, energy independent lipid translocating proteins and the lack of cholesterol.[9] Overall, lipid translocation still remains poorly understood.

Recent evidence has shown that placing a charged molecule in the interior of a lipid bilayer causes structural deformations, which allow water and lipid head groups to enter the hydrophobic interior, to prevent the desolvation of the charged particle.[10–13] The formation of water defects (water present only in one of the bilayer leaflets) and pores (water channel across the entire bilayer) in lipid bilayers has fundamental biological importance. Antimicrobial peptides, as well as cationic penetrating peptides have been shown to induce pore formation.[14,15] Experimentally it was shown that magainin 2 increases the rate of lipid flip-flop, which was correlated to membrane permeabilization.[16] Computer simulations have been used to calculate the free energy of pore formation.[17] By applying an electrical potential across the bilayer, pores have been shown to occur.[18] Similarly, by creating a chemical potential difference across a lipid bilayer, pore formation was observed.[19] The rate of DPPC flip-flop was estimated by calculating the potential of mean force (PMF), and was shown to occur by a pore-mediated mechanism.[10] Computer simulations have provided a unique and relatively consistent view of membrane pore formation.

University of Calgary, department of biological sciences, 2500 University drive, Calgary AB, T2N 1N4. E-mail: tieleman@ucalgary.ca

† This paper is part of a *Soft Matter* themed issue on Membrane Biophysics. Guest editor: Thomas Heimburg.

‡ Nicolas Sapay and W. F. Drew Bennett have equally contributed to the manuscript

We seek a molecular level thermodynamic description for PC lipid flip-flop and desorption. Using molecular dynamics we calculate the free energy for transferring single di12:0-PC (DLPC), di14:0-PC (DMPC), di16:0-PC (DPPC), 16:0, 18:1-PC (POPC), and di18:1-PC (DOPC) lipids from water to the center of model bilayers composed of the respective lipid. We have investigated a series of saturated PC lipids with different lengths of acyl tail, as well as the effect of unsaturated lipid tails. We determine the free energy barrier for PC lipid flip-flop and pore formation from the free energy to move the lipid from equilibrium to the center of the bilayer. Our calculations also provide the free energy required for lipid desorption, which is the excess chemical potential of the phospholipid.

Methods

The partitioning of DLPC, DMPC, POPC, and DOPC in fully hydrated bilayers was studied in four separate sets of simulations. The partitioning of DPPC comes from a previous study using the same force field and parameters.[10] Each bilayer system contained 64 lipids and more than 4000 water molecules. Lipid parameters were derived from the united atom force field of Berger *et al.*[20] Water was modeled with the simple point charge model.[21] Topology files are available at http://moose.bio.ucalgary.ca.

All simulations were carried out with GROMACS 3.3.1.[22] We used a time step of 2 fs. Lennard-Jones and Coulomb potentials were cutoff at 0.9 nm. Long-range electrostatics were treated using the particle mesh Ewald algorithm,[23,24] with a grid spacing of *viz.* 0.1 nm and a real space cutoff of 0.9 nm. The temperature and the pressure were kept constant at 323 K and 1 bar using Berendsen coupling.[25] We used semi-isotropic pressure coupling with a compressibility of 4.5×10^{-5} bar^{-1} and a coupling constant of 2.5 ps for pressure and 0.1 ps for temperature. All lipid bonds were constrained with the LINCS algorithm.[26] Water bonds and angles were constrained with the SETTLE algorithm.[27]

Umbrella sampling was used to calculate the free energy profile for partitioning of DLPC, DMPC, POPC and DOPC into their respective bilayer. A harmonic restraint with a force constant of 3000 kJ mol^{-1} nm^{-2} was applied to the distance between the phosphate of the pulled lipid and the center of mass of the bilayer, in the direction normal to the bilayer plane (z-axis). There was a 0.1 nm spacing between biasing potentials, with a total of 40 simulations for DLPC and DMPC and 50 for POPC and DOPC. In each umbrella window, we had two restrained lipids, one per leaflet, which allowed us to determine two PMFs simultaneously. The phosphates of the two restrained PC lipids were offset by at least 4 nm, so that while the first restrained lipid was at the center of the bilayer, the second was in bulk water. We have shown previously that having two charged molecules spaced at 3.6 nm did not significantly affect its PMF.[11] The weighted histogram analysis method[28] was used to calculate the potentials of mean force (PMFs) from the biased distributions. Each window was equilibrated for 1 ns with a force constant of 1000 kJ mol^{-1} nm^{-2}, then 10 ns with a force constant of 3000 kJ mol^{-1} nm^{-2}. Finally, production simulations were run for 70 ns (DLPC, DMPC), 20 ns (POPC and DOPC). As two lipids are restrained for each window, the standard error can be determined from the two PMFs. We judged the length of the simulations on the convergence of the two leaflets PMFs.

Trajectory analysis and visualization were performed with the tools included in the GROMACS package or VMD 1.8.6.[29] Image rendering was done with POV-Ray 3.6.1 (www.povray.org).

Results

Equilibrium structural properties

Density profiles for the DLPC, DMPC, DPPC, POPC and DPPC bilayers are shown in Fig. 1A. As expected, the profiles have a similar shape, and in general, the bilayer becomes thicker as the number of carbons in the acyl tail increases. For the saturated lipids, DLPC, DMPC, and DPPC, the area per lipid A decreases as the number of carbons in the acyl tail increases ($A_{DLPC} = 0.72$ nm^2, $A_{DMPC} = 0.71$ nm^2, $A_{DPPC} = 0.69$ nm^2). Increasing the level of unsaturation in the lipid tails, by adding one double bond, for POPC, and two for DOPC, increases the area per lipid compared to DPPC ($A_{POPC} = 0.69$ nm^2, $A_{DOPC} = 0.73$ nm^2). The areas per lipid estimated from our simulations are higher than the experimental values (at 323 K: $A_{DLPC} = 0.671$ nm^2,[30] $A_{DMPC} = 0.654$ nm^2,[30] $A_{DPPC} = 0.633$ nm^2,[30] $A_{POPC} = 0.683$ nm^2;[31] at 303 K: $A_{DOPC} = 0.724$ nm^2[32]), but the expected trend in the bilayers structural properties is correct.

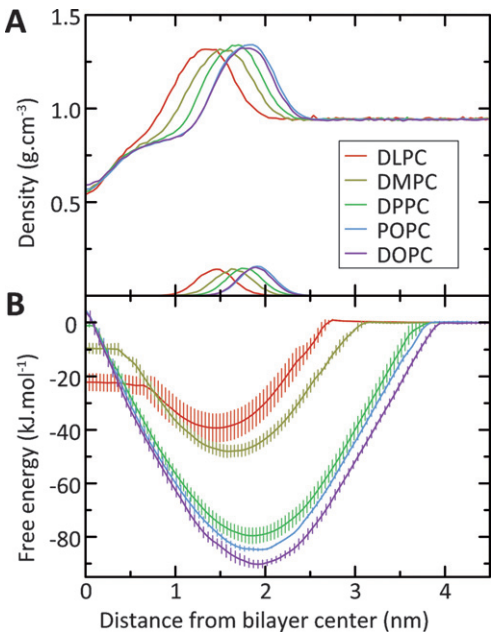

Fig. 1 (A) Partial density profiles for the series of lipid bilayers at equilibrium. Shown are the total system density and the phosphate density. (B) Lipid PMFs for the series of bilayers. We restrained the phosphate of the PC lipids for umbrella sampling, so the distance refers to the position of the phosphate with respect to the bilayer center. Error bars represent the standard error from the two leaflets PMFs. The energy was arbitrarily set to zero in the bulk water for ease of comparison, not to suggest the lipids have the same free energy of hydration. The color code is the same for both panels.

Lipid PMFs

Fig. 1B shows PMFs for transferring a DLPC, DMPC, DPPC, POPC, and DOPC molecule from water to the center of the respective bilayer. The PMFs describe the free energy required for deviations of individual lipids from their equilibrium position along the normal to the plane of the bilayer. The trough in the PMF is the equilibrium position of the PC lipid in the bilayer. As the bilayer gets thicker, the trough of the PMF moves farther from the bilayer center and corresponds to the position of the partial density of the phosphate at equilibrium (Fig. 1A). There is a steep slope in free energy as the phosphate moves toward the bilayer center, due to the bulky zwitterionic head group of the PC lipid interacting with the hydrophobic interior of the bilayer. A similar steep slope is observed when the lipid moves into bulk water, as expected from the low solubility of phospholipids in water. A plateau appears when the lipid stops interacting with the bilayer, and therefore is the free energy of the lipid diffusing in bulk water.

Lipid flip-flop

We assume the free energy at the center of the bilayer is the primary free energy barrier for flip-flop. In general, the free energy barrier for flip-flop increases as the bilayer becomes thicker: ΔG_{flop} for DLPC, DMPC, DPPC, POPC, and DOPC are equal to 16, 40, 80, 89, and 94 kJ mol^{-1}.

Transferring the PC head group into the hydrophobic interior of the bilayer causes water defect and pore formation; water and other PC head groups move into the bilayer core to keep the lipid solvated. Fig. 2A shows snapshots of the systems when a lipid is restrained at the center of the bilayer, *i.e.* when $z = 0$ nm in the PMFs. Our series of membranes have different structural properties, they respond differently to having a PC head group in there interior.

We observe a large water pore when the phosphate of DLPC is at the bilayer center (Fig. 2). The plateau near the bilayer center in the PMF for DLPC corresponds to the location where pore formation occurs. For example, at $z = 0.7$ nm only a water defect through one leaflet of the bilayer is present, while at $z = 0.5$ nm a water pore forms. We estimate the pore radius for DLPC to be 0.95 nm at the center of the bilayer, from the two-dimensional density map of water (Fig. 2B).

Examining the DMPC PMF, we observe a similar plateau and corresponding water pore near the center of the bilayer. Compared to DLPC, the plateau is shorter, and the free energy barrier is 2.3 times larger. As well, the pore radius is smaller with a value of 0.86 nm.

The PMF for DPPC does not contain a plateau (Fig. 1B), although we do observe pore formation at the bilayer center (Fig. 2). The pore only appears when $z = 0$ nm and occasionally when $z = 0.1$ nm, but not for larger z coordinates. The pore radius at the center of the bilayer is 0.55 nm, smaller than for DMPC and DLPC.

For POPC and DOPC, we do not observe pores (Fig. 2A), nor do the PMFs display plateaus. This suggests more energy is required for pore formation and subsequently flip-flop. In contrast with the saturated lipids, the phosphate density is null when DOPC is at the center of the bilayer (Fig. 2B), while the water density is appreciable (Fig. 2C). This suggests that the mechanical properties of DOPC make it more favorable for water to enter the hydrophobic bilayer interior, in direct contact with the acyl chains, rather than have the bilayer deform, and allow their phosphates into the bilayer interior.

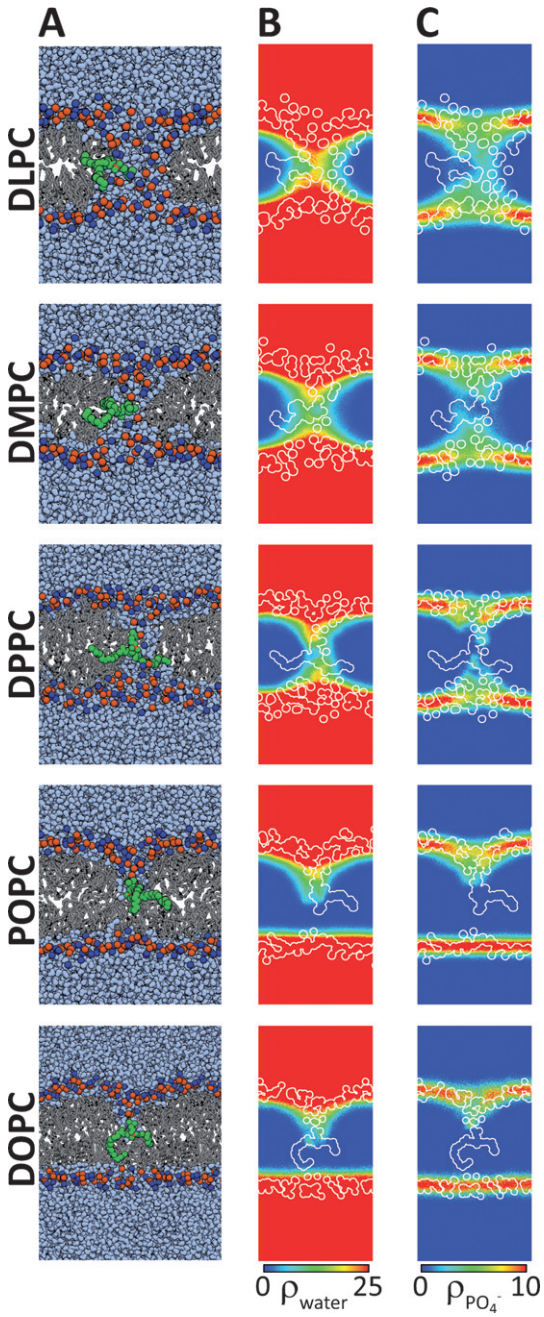

Fig. 2 Water pores or defects formed when the PC lipid is restrained at the center of each bilayer. (A) Snapshots of the systems. Water is in light blue, the restrained lipid is in green, the other lipids are in grey, the nitrogen atoms are in dark blue and the phosphorus atoms are in orange. (B) Two-dimensional water density map of each system (in atom nm^{-3}). (C) Two-dimensional phosphate density map of each system (in atom nm^{-3}). The pulled lipids, nitrogen and phosphorus atoms are represented to scale as a white line in both density maps.

Water pore characterization

To quantify the water defect and pore formation we have determined the number of water molecules that penetrate into the hydrophobic interior of the bilayer, as a function of the position of the pulled lipid (Fig. 3A). When the lipid is at equilibrium there are between 5 and 10 water molecules in the bilayer interior. As we move the lipid toward the bilayer center, there is an increase in the number of water molecules, corresponding to the formation of a water defect. DLPC and DMPC display large increases in the number of water molecules in the interior of the bilayer as a water pore forms. DLPC has a maximum number of waters in the bilayer interior at z = 0.25 nm. The maximum for DMPC is at the bilayer center. For the other lipids, there is a steady increase in the water within the interior from equilibrium to the center of the bilayer. For, POPC and DOPC, the water defect contains approximately 16 waters, *i.e.* about 2 times less than in the DLPC pore.

The number of hydrogen bonds to the pulled lipid as it is transferred from water into the center of the bilayer was also determined (Fig. 3B). The maximum number of hydrogen bonds is when the PC lipid is in bulk water. Transferring the lipid from water into its equilibrium position, there is a decrease in the number of hydrogen bonds. We do not observe a plateau at the lipids equilibrium position. The number of hydrogen bonds decreases as it is moved into the bilayer interior, but never reaches zero, meaning the PC head group is never fully desolvated. Instead, it is stabilized by between 5 and 6 hydrogen bonds for DPPC, POPC and DOPC (Fig. 2A). In contrast, for DLPC and DMPC the number of hydrogen bonds increases to greater than 6 hydrogen bonds, as a water pore forms.

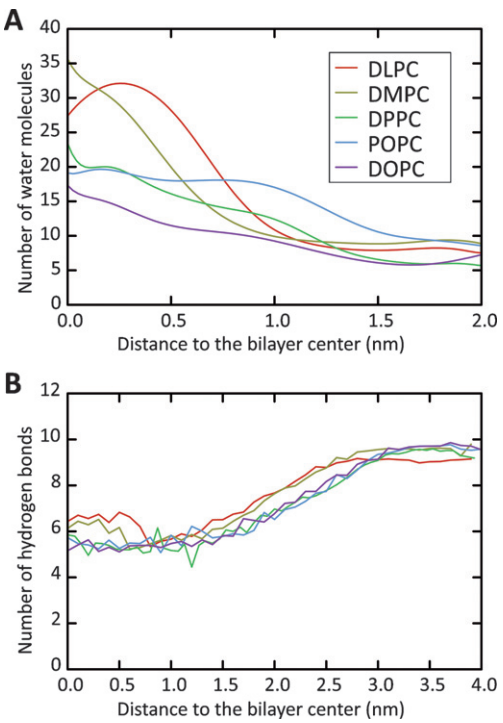

Fig. 3 Characterization of the water pore or defect formed during lipid flip-flop. (A) The number of water molecules within the hydrophobic interior of the bilayers as a function of the distance between the restrained phosphate and the bilayer center of mass. The interior is defined as the distance between the ester density peaks. The curves were smoothed with a Bezier scheme to limit the background noise. The peaks and drops at $z = 0$ nm for DLPC, DMPC and DPPC are not significant. They are due to the large fluctuations of the number of water molecules and the smoothing scheme. (B) The number of hydrogen bonds between the restrained lipid and water as a function of the distance between the restrained phosphate and the bilayer center of mass. The definition of hydrogen bonds is based on geometric criteria (distance <0.35 nm, angle <30°). The color code is the same for both panels.

Water PMFs

As we observed large structural deformations of the bilayers for lipid flip-flop, we wanted to investigate the translocation of a small polar molecule that did not cause deformations. Without deformations, the chemical environment of the interior of all the bilayers should be similar, and therefore a small molecules free energy of transfer from bulk water to center of the bilayers should be consistent. As a control, we have determined PMFs for transferring a single water molecule from bulk solution into the center of the bilayers (Fig. 4A). As expected, the PMFs are flat in bulk water, and increase as the water molecule moves into the interior of the bilayer. The steep slope in the water PMFs plateau near the bilayer center. Within the standard error, the water molecule has the same free energy of transfer in the DLPC, DPPC, POPC, and DOPC bilayers.

We have determined the number of hydrogen bonds formed to the pulled water as it is transferred into the bilayer interior (Fig. 4B). Contrary to the PC PMFs, which plateau when a pore forms, the water PMFs plateau when the water becomes

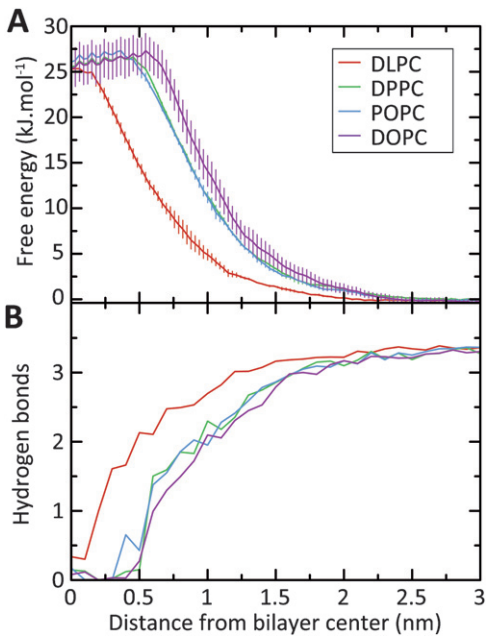

Fig. 4 (A) PMFs for water partitioning in the series of lipid bilayers. Error bars are the standard error from the two leaflets individual PMFs. (B) Hydrogen bonds to the pulled water molecule as it is moved from bulk water to the bilayer center. The color code is the same for both panels.

desolvated; the average number of hydrogen bonds drops to near zero. Once the water is desolvated it freely diffuse across the hydrophobic interior of the bilayer.

Desorption

The free energy required for desorption is the free energy difference between equilibrium and bulk water (Fig. 1B). Once the lipid stops interacting with the bilayer, the PMF plateaus, indicating a constant free energy for moving the lipid through bulk water. The free energy of desorption for DLPC, DMPC, DPPC, POPC, and DOPC are equal to 39, 48, 80, 85, and 90 kJ mol^{-1}. In general, as the number of carbons on the acyl tail increases the free energy for desorption increases.

For all the lipids, we observe a critical distance at which the tails stop interacting with the bilayer. To quantify this phenomenon, we measured the head to tail distance for the pulled lipid in each umbrella window (Fig. 5). As expected, this distance increases as the acyl chains get longer; the DLPC head-to-tail distance is shorter than DPPC. At equilibrium, the tails are extended, resulting in a large head-to-tail distance. As the lipid is transferred from equilibrium into bulk water, the head-to-tail distance increases. The lipid becomes extended to prevent the acyl tails being exposed to bulk water. At a critical distance from equilibrium, we observed that the PC lipid tails stopped interacting with the bilayer and folded up into bulk water, to minimize exposure of the hydrophobic tails to water. This position directly corresponds to the plateau of the PMF in bulk water (Fig. 1B). For POPC, the tail fluctuates between inserted in the bilayer and folded up in bulk water, in adjacent umbrella windows.

Discussion

The areas per lipid for all of our bilayers are higher than experimental values. The simulation parameters have been shown to affect the area per lipid and the correct area per lipid can be obtained using any force field with a particular set of parameters.[33] We have shown that a cholesterol PMF in a DPPC bilayer is not significantly affected by using constant area and at

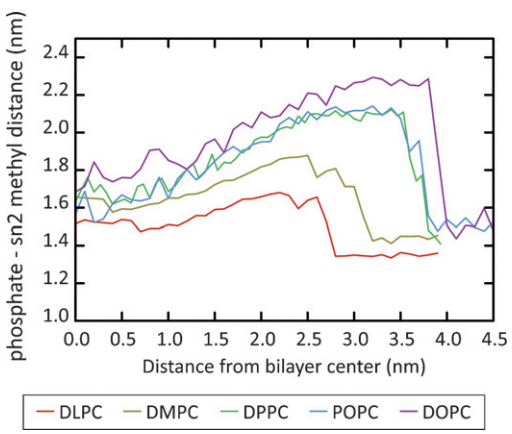

Fig. 5 Distance between the phosphate and the methyl of the sn-2 acyl chain for the restrained lipids as a function of the distance between the phosphate and the bilayer center of mass.

±10% area per lipid (W. F. D. Bennett, D. P. Tieleman, unpublished work). This suggests the exact area per lipid is not crucial for free energies of lipid transfer.

Pores and defects

The lipid PMFs have a steep slope as we transfer the head group into the interior of the bilayer (Fig. 1B). The increase in free energy is correlated to the formation of a water defect, which becomes larger as the lipid is transferred farther into the bilayer. It is energetically more favorable for the bilayer to deform and allow a water defect than for the PC lipid head group to become desolvated. At a critical distance from the center of the DLPC, DMPC, and DPPC bilayers, the water defect becomes a pore, with water penetrating into the hydrophobic interior of the bilayer from both leaflets (Fig. 2). Once a pore forms, the restrained lipid can freely diffuse across the interior of the bilayer from one leaflet to the other. Our free energy calculations allow us to extract the free energy of pore formation in membranes as well as the free energy barrier for flip-flop. It is interesting that pore formation is strongly correlated with the plateau in the PMF. Therefore, the free energy for pore formation might be an intrinsic property of the bilayer, and largely independent of the method used to create the pore. Indeed, the structure and dynamics of our observed water defects and pores are consistent with many other simulations.[17–19,34] Of particular interest with respect to our current focus, is the work of Wohlert *et al.* who investigate the free energy of pore formation with the pore radius as the reaction coordinate.[17] For a DPPC bilayer, the PMF for pore formation with a radius of <0.3 nm had a quadratic shape, and a free energy cost of 75–100 kJ mol^{-1}.[17]

The structure and fluidity of the membrane directly affect water pore and defect formation. As expected, the shorter lipids formed pores much easier than the longer lipids. This resulted in the large increase in ΔG_{flop} that we observed for DOPC (90 kJ mol^{-1}) compared to DLPC (16 kJ mol^{-1}). Fig. 2 shows that the structure of the hydrophobic pore is different for all of the bilayers. For example, DLPC has a large pore radius, with water and phosphate density near the bilayer center. The pore in DPPC is much smaller, with an increased curvature of the pore wall and little phosphate density at the bilayer center. Although we do not see pore formation in the DOPC bilayer, the water defect displays the same trend, with increased defect curvature and reduced pore radius (*i.e.* 0 nm). From the structure of the observed pores and defects, it is clear that the bilayers bend to accommodate the zwitterionic lipid.

For DPPC, we observed a pore only at the bilayer center. We have shown previously that adding 40 mol% cholesterol to a DPPC bilayer, caused the free energy barrier for DPPC flip-flop to increase to 110 kJ mol^{-1}, and prevented pore formation.[35] At the center of the 40 mol% bilayer, we observed a plateau in the PMF, which corresponded to cessation of the water defect, and four or five water molecules forming a solvation 'bubble' around the head group of DPPC. Cholesterol increases the thickness and reduces the fluidity of lipid bilayers. Therefore, the increased free energy barrier for DPPC flip-flop in the 40 mol% cholesterol bilayer follows the same trend as the present results.

The water PMFs served as a control showing that the differences we observe for the PC lipid PMFs are due to bilayer

deformations. The free energy of transfer for a small, polar molecule, which did not form defects or pores at the bilayer center, was consistent for the DLPC, POPC, DPPC, and DOPC bilayers (Fig. 4). In addition, the water PMFs demonstrated that when a polar molecule becomes desolvated, the PMF plateaus. We have observed similar behavior in the investigation of the polar and charged amino acid side chains partitioning in a DOPC bilayer.[11,34] Water defect formation caused the PMFs of the polar and charged side chains to have a steep slope. The PMFs flattened when the defect broke, when it was energetically more favorable to desolvate the side chain than to deform the bilayer. The slope for all the side chains PMFs was similar, but the distance the defect broke, and the length of the plateau depended on the particular side chain. This supports the idea that defect formation dominates the slope of the PMF for polar and charged molecules.

Our present results provide new insight into biological membranes' function as selective barriers. Lipid bilayers are extremely flexible and dynamic, which allow them to adjust their structure to accommodate charged molecules within their hydrophobic interior. These structural deformations are critical determinants in the shape of PMFs and the height of free energy barriers for molecules translocating across lipid membranes. Once a water defect either breaks, or expands into a pore, the free energy of transfer across the bilayer becomes zero. The lipid composition of the respective bilayer would affect the energy required for water defect and pore formation, and consequently the permeation of polar and charged molecules.

Flip-flop rates

The rate of passive lipid flip-flop can be estimated from ΔG_{flop}. We assume the transition state for flip-flop is when the PC lipid is at the bilayer center. This assumption is supported by the correlation of pore formation and the free energy plateau. Therefore we can estimate the rate of pore formation, k_f, using:

$$\frac{k_f}{k_d} = e^{-\Delta G/RT} \quad (1)$$

where k_d is the rate of pore dissipation. Due to the large free energy barrier, we assume that the rate for the phosphate of the PC lipid to reach the interior of the bilayer will dominate all other considerations. Obtaining an accurate estimate for the rate of pore dissipation from simulation is non-trivial. We attempted to measure k_d from 50 independent simulations of a DMPC bilayer with a pre-formed pore (data not shown). However, this attempt failed as the phenomenon is largely stochastic, with some pores remaining after 50 ns and others dissipating in nanoseconds. Gurtovenko and Vattulainen found similar results using pre-formed pores in a DMPC bilayer, with metastable pores lasting from 35 to 200 ns.[36] Eqn 1 implies that an increase in the rate of flip-flop by 1 order of magnitude decreases ΔG_{flop} by 5.7 kJ mol^{-1}. This is approximately the same magnitude as the standard error of the PMFs.

Instead of attempting a more rigorous estimate of the rate, we have used the same range of k_d values (10–100 ns) for all the bilayers, and the same assumptions as in ref. 10. We find the rates for DLPC, DMPC, DPPC, POPC and DOPC flip-flop occur on the microsecond, second, hour, hour, and day timescales, respectively. We did not observe pore formation in the POPC and DOPC bilayers, and therefore we are unsure about their transition state and free energy barrier for flip-flop.

In general, comparison to experiment is difficult as literature values span large ranges depending on experimental procedure, such as the use of fluorescent probes. The difference in temperature used in many of the experiments and our study also impedes direct comparison. A recent study of DMPC, DPPC, and DSPC flip-flop in planar supported bilayers, using sum-frequency vibrational spectroscopy showed Arrhenius behavior for flip-flop, indicating an exponential dependence of the temperature on the rate.[37] The rate of DMPC flip-flop was found to be faster than DPPC and DSPC, although all the rates were determined in gel state bilayers.[37] TEMPO labeled DPPC had an order of magnitude slower rate of flip-flop, compared to DPPC, showing the use of labeled analogs has a large effect on many experimental values for lipid flip-flop rates.[37] At the main phase transition temperature of DMPC and DPPC the rate of flip-flop of NBD-labeled analogs was increased compared to the gel and liquid-crystalline phases.[38] Again, the rate of flip-flop in the DMPC bilayer was faster than in the DPPC bilayer.[38] The rate of NBD-PE flip-flop was shown to be dependent on the number of double bonds in the PC lipids acyl tail, with much faster flip-flop in poly-unsaturated bilayers.[39] Of interest to our study, it was shown that NBD-PE flip-flop was faster in DOPC bilayers compared to DPPC, but the low temperature used (25 °C), meant that the DPPC bilayer was in the gel phase.[39] Our results show that flip-flop of DLPC would be orders of magnitude faster than DPPC flip-flop. Our estimations are crude, but we do not focus on specific values, other than to note the value for DPPC was previously shown to be well within the experimental range of rates (1 to 90 hours).[10] The extremely fast flip-flop we predict for the DLPC and DMPC bilayers does seem somewhat unrealistic, and may point to possible force field issues. We predict a rate decrease as we increase the number of double bonds, which disagrees with the results of[39] and the predicted effect of the increased fluidity caused by double bonds. This may be due to the double bond parameters we have used, but the difference in temperature and phases, makes direct comparison with[39] impossible. It would be interesting to repeat our calculations on poly-unsaturated acyl tails or to determine experimental rates of unlabeled lipids in single component bilayers all at the same temperature. In retrospect we should have used the same length of acyl tails, as our unsaturated tails are also longer (18:1C) than the saturated DPPC bilayer (16:0C).

Biologically, the large discrepancy we observe in the free energy barriers for flip-flop suggests differential rates of lipid flip-flop between different cellular organelles. In thin, fluid ER membranes, flip-flop would be orders of magnitude faster than in plasma membranes that are more rigid. Much remains unknown about lipid translocation, which is biologically important.

Chemical potential

The free energy for desorption relies on the equilibrium stability of the lipid in the bilayer, in addition to the solubility of the lipid in water. We can equate the free energy of desorption to the excess chemical potential of the lipid in the bilayer compared to bulk water. The chemical potential of a lipid is a crucial

thermodynamic parameter and determines lipid partitioning, and is therefore important for phase behavior and domain formation in membranes. For instances, the critical micelle concentration (CMC) of a lipid is directly related to the excess chemical potential of the lipid in bulk water compared to a micelle,

$$\mu - \mu_0 = RTln(CMC)$$

The CMC of DLPC, DMPC, and DPPC are 280, 94, and 0.3 nM, which equate to excess chemical potentials of 51, 54, and 69 kJ mol^{-1}.[40] Note that CMCs have to be converted to mole fraction units, *i.e.* divided by 55.5 M. Our calculated excess chemical potential for DLPC, DMPC, and DPPC were 39, 48, and 80 kJ mol^{-1}, which demonstrate the correct qualitative trend. It is surprising that we underestimate the chemical potential of DLPC and DMPC, but over estimate DPPC.

Obtaining correct thermodynamic data, such as chemical potentials, is important for molecular dynamics simulations. Our results show that current force fields can produce reasonable results for the chemical potential of PC lipids. For more complex biological phenomena, such as lateral domain formation, subtle discrepancies in chemical potentials likely have very large and unpredictable effects. In the future, a new generation of lipid force fields might be parameterized to reproduce thermodynamic phase data.

Conclusion

We have calculated free energy profiles for the movement of a series of phospholipids normal to the plane of lipid bilayers. The free energy to move the PC lipid from equilibrium to the center of the bilayer is the free energy barrier for flip-flop. We found that the composition of the bilayer and therefore the structure of the bilayer had a large effect on the free energy barrier, and therefore on the rate of flip-flop. Thinner bilayers, such as DLPC, had lower free energy barriers (16 kJ mol^{-1}), compared to thicker bilayers, like DPPC (80 kJ mol^{-1}). We observed large water pores for the shorter lipids, which became smaller as we increased the bilayer thickness. We equated the free energy difference between the equilibrium position of the PC lipid, and bulk water to the excess chemical potential of the lipid. As expected, as we increased the number of carbons in the acyl tails the chemical potential decreased, *i.e.* it became more unfavorable to remove the lipid from the bilayer. In general, the composition of bilayers strongly affects important thermodynamic properties, which have broad implications on biological membranes.

List of abbreviations

DLPC	dilauroylphosphatidylcholine
DMPC	dimyristoylphosphatidylcholine
DPPC	dipalmitoylphosphatidylcholine
DOPC	dioleoylphosphatidylcholine
POPC	1-palmitoyl-2-oleoyl-phosphatidylcholine
MD	molecular dynamics
PMF	potential of mean force
ER	endoplasmic reticulum

Acknowledgements

WFDB is supported by studentships from the Natural Science and Engineering Research Council (NSERC, Canada) and the Alberta Heritage Foundation for Medical Research (AHFMR). DPT is an AHFMR Senior Scholar and Canadian Institutes for Health Research New Investigator. This work was supported by NSERC. Calculations were done in part on WestGrid facilities.

References

1 G. van Meer, D. R. Voelker and G. W. Feigenson, *Nat. Rev. Mol. Cell Biol.*, 2008, **9**, 112–124.
2 B. De Kruijff and E. J. Van Zoelen, *Biochim. Biophys. Acta*, 1978, **511**, 105–115.
3 R. D. Kornberg and H. M. McConnell, *Biochemistry*, 1971, **10**, 1111–1120.
4 W. C. Wimley and T. E. Thompson, *Biochemistry*, 1990, **29**, 1296–1303.
5 D. L. Daleke, *J. Lipid Res.*, 2003, **44**, 233–242.
6 M. A. Kol, B. de Kruijff and A. I. de Kroon, *Semin. Cell Dev. Biol.*, 2002, **13**, 163–170.
7 M. A. Kol, A. I. de Kroon, D. T. Rijkers, J. A. Killian and B. de Kruijff, *Biochemistry*, 2001, **40**, 10500–10506.
8 M. A. Kol, A. van Dalen, A. I. de Kroon and B. de Kruijff, *J. Biol. Chem.*, 2003, **278**, 24586–24593.
9 M. A. Kol, A. N. C. van Laak, D. T. S. Rijkers, J. A. Killian, A. I. P. M. de Kroon and B. de Kruijff, *Biochemistry*, 2003, **42**, 231–237.
10 D. P. Tieleman and S. J. Marrink, *J. Am. Chem. Soc.*, 2006, **128**, 12462–12467.
11 J. L. MacCallum, W. F. D. Bennett and D. P. Tieleman, *Biophys. J.*, 2008.
12 S. Dorairaj and T. W. Allen, *Proc. Natl. Acad. Sci. U. S. A.*, 2007, **104**, 4943–4948.
13 J. A. Freites, D. J. Tobias, G. von Heijne and S. H. White, *Proc. Natl. Acad. Sci. U. S. A.*, 2005, **102**, 15059–15064.
14 H. Leontiadou, A. E. Mark and S. J. Marrink, *J. Am. Chem. Soc.*, 2006, **128**, 12156–12161.
15 H. D. Herce and A. E. Garcia, *Proc. Natl. Acad. Sci. U. S. A.*, 2007, **104**, 20805–20810.
16 K. Matsuzaki, O. Murase, N. Fujii and K. Miyajima, *Biochemistry*, 1996, **35**, 11361–11368.
17 J. Wohlert, W. K. den Otter, O. Edholm and W. J. Briels, *J. Chem. Phys.*, 2006, **124**, 154905.
18 D. P. Tieleman, *BMC Biochem.*, 2005, **5**, 10.
19 A. A. Gurtovenko and I. Vattulainen, *J. Am. Chem. Soc.*, 2005, **127**, 17570–17571.
20 O. Berger, O. Edholm and F. Jahnig, *Biophys. J.*, 1997, **72**, 2002–2013.
21 H. J. C. Berendsen, J. P. M. Postma, W. F. van Gunsteren and J. Hermans, *Interaction Models for Water in Relation to Protein Hydration.*, D. Reidel, Dordrecht, The Netherlands, 1981.
22 D. Van der Spoel, E. Lindahl, B. Hess, G. Groenhof, A. E. Mark and H. J. C. Berendsen, *J. Comput. Chem.*, 2005, **26**, 1701–1718.
23 T. Darden, D. York and L. Pedersen, *J. Chem. Phys.*, 1993, **98**, 10089–10092.
24 U. Essmann, L. Perera, M. L. Berkowitz, T. Darden, H. Lee and L. G. Pedersen, *J. Chem. Phys.*, 1995, **103**, 8577–8593.
25 H. J. C. Berendsen, J. P. M. Postma, W. F. Vangunsteren, A. Dinola and J. R. Haak, *J. Chem. Phys.*, 1984, **81**, 3684–3690.
26 B. Hess, H. Bekker, H. J. C. Berendsen and J. G. E. M. Fraaije, *J. Comput. Chem.*, 1997, **18**, 1463–1472.
27 S. Miyamoto and P. A. Kollman, *J. Comput. Chem.*, 1992, **13**, 952–962.
28 S. Kumar, D. Bouzida, R. H. Swendsen, P. A. Kollman and J. M. Rosenberg, *J. Comput. Chem.*, 1992, **13**, 1011–1021.
29 W. Humphrey, A. Dalke and K. Schulten, *J. Mol. Graphics*, 1996, **14**, 33.
30 H. I. Petrache, S. W. Dodd and M. F. Brown, *Biophys. J.*, 2000, **79**, 3172–3192.

31 G. Pabst, M. Rappolt, H. Amenitsch and P. Laggner, *Phys. Rev. E.*, 2000, **62**, 4000–4009.
32 J. F. Nagle and S. Tristram-Nagle, *Biochim. Biophys. Acta-Rev. on Biomem.*, 2000, **1469**, 159–195.
33 C. Anezo, A. H. de Vries, H. D. Holtje, D. P. Tieleman and S. J. Marrink, *J. Phys. Chem. B.*, 2003, **107**, 9424–9433.
34 J. L. MacCallum, W. F. D. Bennett and D. P. Tieleman, *J. Gen. Physiol.*, 2007, **129**, 371–377.
35 W. F. D. Bennett, J. L. MacCallum and D. P. Tieleman, *J. Am. Chem. Soc.*, 2009, **131**, 1972–1978.
36 A. A. Gurtovenko and I. Vattulainen, *J. Phys. Chem. B.*, 2007, **111**, 13554–13559.
37 J. Liu and J. C. Conboy, *Biophys. J.*, 2005, **89**, 2522–2532.
38 K. John, S. Schreiber, J. Kubelt, A. Herrmann and P. Muller, *Biophys. J.*, 2002, **83**, 3315–3323.
39 V. T. Armstrong, M. R. Brzustowicz, S. R. Wassall, L. J. Jenski and W. Stillwell, *Arch. Biochem. Biophys.*, 2003, **414**, 74–82.
40 G. Cevc and D. Marsh, in *Phospholipid Bilayers: Physical Principles and Models*, Wiley, New York, 1987.

